Direct empirical proof of dark matter?

Masaki Mori

Reference:
D. Clowe et al., astro-ph/0608407
J.W. Moffat, astro-ph/0608675

ICRR CANGAROO Group Internal Seminar, 05-OCT-2006

Bergstroem and Goobar, "Cosmology and Particle Astrophysics" (2nd ed., 2004)

Bending of light

There is another way to derive the law of deflection which is of general applicability. This starts from a general relativistic version of Fermat's principle, which states that light-rays follow paths which minimize the travel time. From the optics point of view, the gravitational potential φ causes a time delay (called the Shapiro delay) which can be represented by a refractive index

$$n = 1 - 2\varphi \tag{5.13}$$

so that light travels slower than c by a factor n, $v_{eff} = c/n \simeq c(1-2|\varphi|)$. Just as in optics, the deflection is the integral of the gradient of n perpendicular to the direction of propagation, along the light path:

$$\Delta\phi = -\int \nabla_\perp n dl = 2\int \nabla_\perp \varphi dl \tag{5.14}$$

Returning to our example of a point mass, the Newtonian potential for a light-ray travelling along the y axis in the xy-plane is given by

$$\varphi(b,y) = \frac{-GM}{\sqrt{b^2+y^2}} \tag{5.15}$$

which inserted into (5.14) gives $\Delta\phi = 4GM/b$ as before.

須藤靖(2005)

重力レンズの分類

- 光線は重力場によって曲げられる
  - 天体が多重像をつくる(強い重力レンズ)
  - 天体の形状が変形を受ける(弱い重力レンズ)
  - 天体の見かけの明るさが増光する(マイクロレンズ)

観測的宇宙論の進化論 72

http://www.nro.nao.ac.jp/%7Edeguchi/kagoshima/index.html

Theory of gravitational lensing

Lensing by a distand star (Refsdal 1964, Liebes 1964)

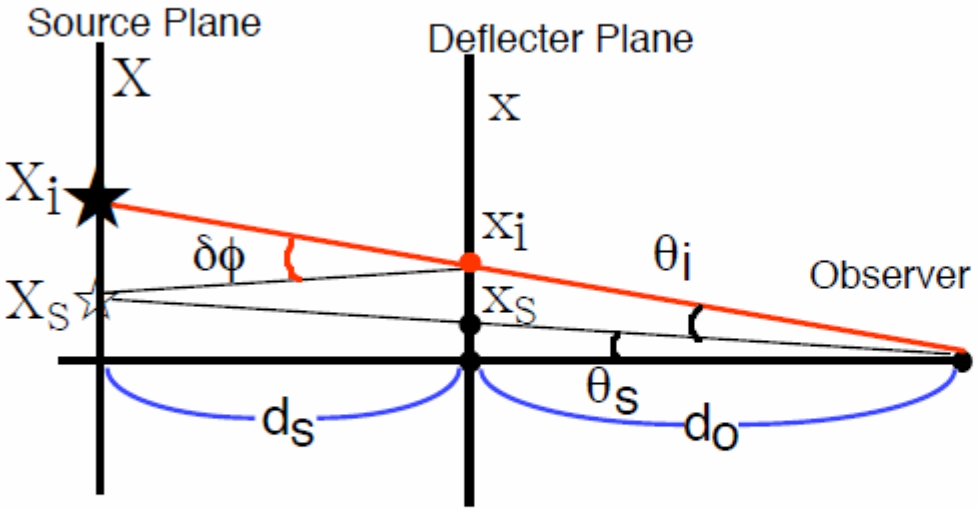

$x_S = X_S * d_o/(d_s+d_o)$

$x_i = X_i * d_o/(d_s+d_o)$

$d \equiv d_s * d_o/(d_s+d_o)$

Shwartzchild Radius :

$r_g = 2\,GM/\,c^2$

Lens Equation: $\delta\phi = 4\,GM/\,(x_i\,c2\,) = 2\,r_g\,/x_i$

$\delta\phi = (X_i - X_S)\,/d_s = (d_s+d_o)(x_i - x_S)/(d_s * d_o)$

Wikipedia.org

Simulation of gravitational lensing (1)

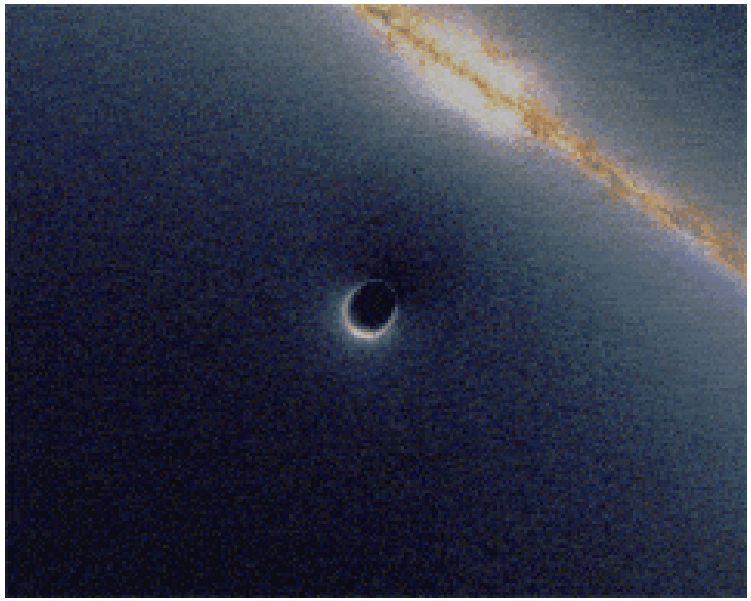

Animated simulation of gravitational lensing caused by a Schwarzschild black hole going past a background galaxy. A secondary image of the galaxy can be seen within the black hole Einstein ring on the opposite direction of that of the galaxy. The secondary image grows (remaining within the Einstein ring) as the primary image approaches the black hole. The surface brightness of the two images remain constant, but their angular size vary, hence producing an amplification of the galaxy luminosity as seen from a distant observer. The maximum amplification occurs when the background galaxy (or in the present case a bright part of it) is exactly behind the black hole.

http://www.ascii.co.jp/pb/ascii/odyssey/index.html

Simulation of gravitational lensing (2)

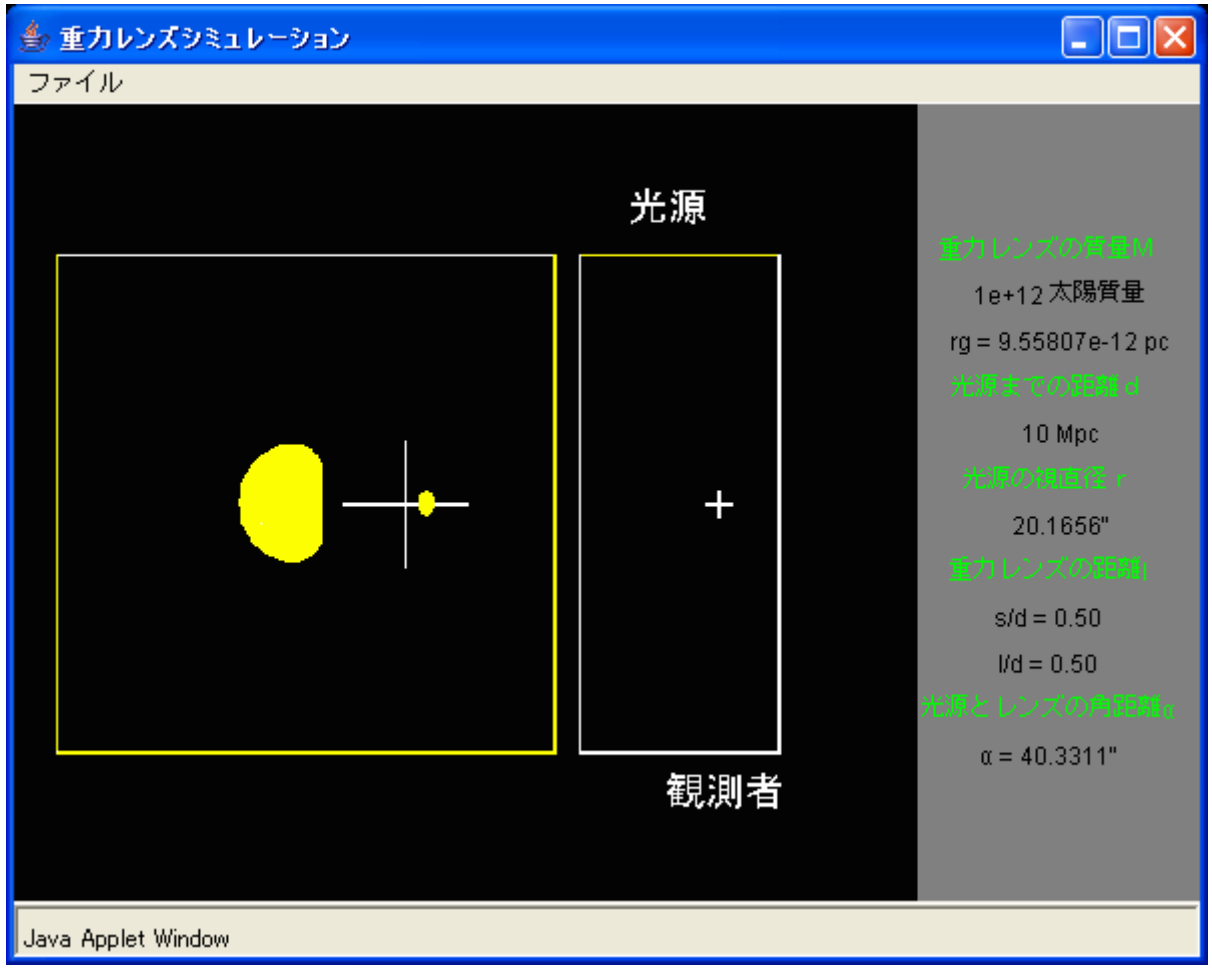

http://www.astro.ucla.edu/~wright/cluster-lensing.html

Simulation of gravitational lensing (3)

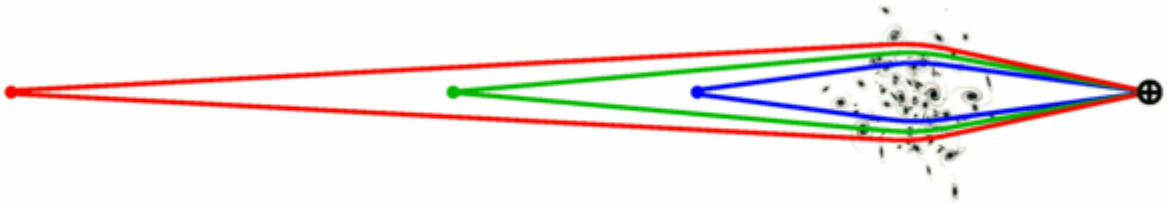

Galaxy cluster

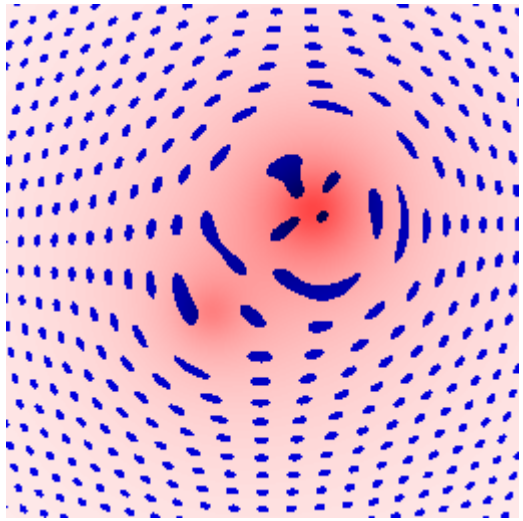

This animation shows the view we would have looking at the sky through a galaxy cluster with two mass concentrations (the pink shading indicates the projected mass density) which is lensing a background field of faint blue galaxies.

Inada et al., Nature 426, 781 (2004)

Example of strong lensing: SDSS J1004+4112

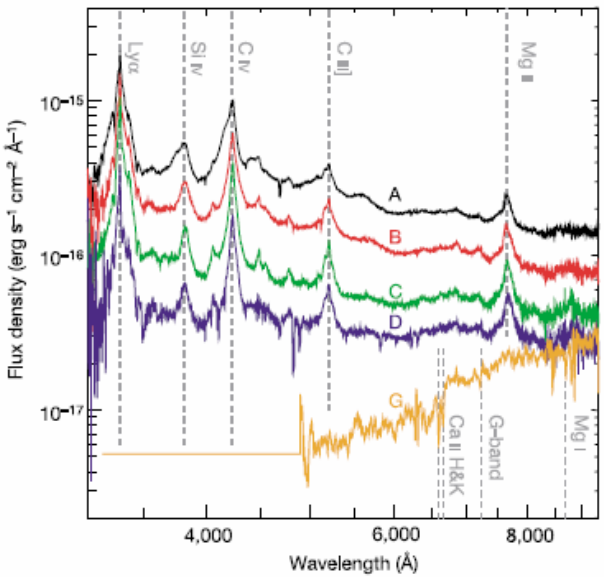

Figure 1 The Keck spectra of the four quasar components A–D, and the brightest galaxy G in the lensing cluster. See Fig. 2 for these identifications (A–D, and G). The data were taken using the Low-Resolution Imaging Spectrometer[29] of the Keck I telescope. The exposure times were 900 s for each component. The dispersion is 1.09 Å pixel^{-1}. The data were reduced in a standard method using IRAF (IRAF is the image reduction and analysis facility, distributed by the National Optical Astronomy Observatories). The black solid line, the red solid line, the green solid line and the blue solid line represent the spectra of components A, B, C and D, respectively. The vertical grey dashed lines with labels at the top of the figure (3,323.6 Å, 3,818.7 Å, 4,235.1 Å, 5,218.5 Å and 7,651.8 Å) represent the positions of emission lines of the respective ions redshifted to $z = 1.734$ of Lyα (1,215.67 Å), Si IV (1,396.76 Å), C IV (1,549.06 Å), C III] (1,908.73 Å) and Mg II (2,798.75 Å), respectively. All emission lines are clearly at the same redshift. The orange solid line represents the Keck spectrum of component G at the same dispersion. The exposure time was also 900 s for component G. The vertical thinner grey dashed lines with labels at the lower right of the figure (6,608.2 Å, 6,666.7 Å, 7,231.0 Å, and 8,694.0 Å) represent the positions of absorption lines of the respective ions redshifted to $z = 0.680$ of Ca II H&K (3,933.7 Å and 3,968.5 Å), G-band (4,304.4 Å), and Mg I B-band (5,175.3 Å), respectively. There are no data below ~4,900 Å in the spectrum of component G.

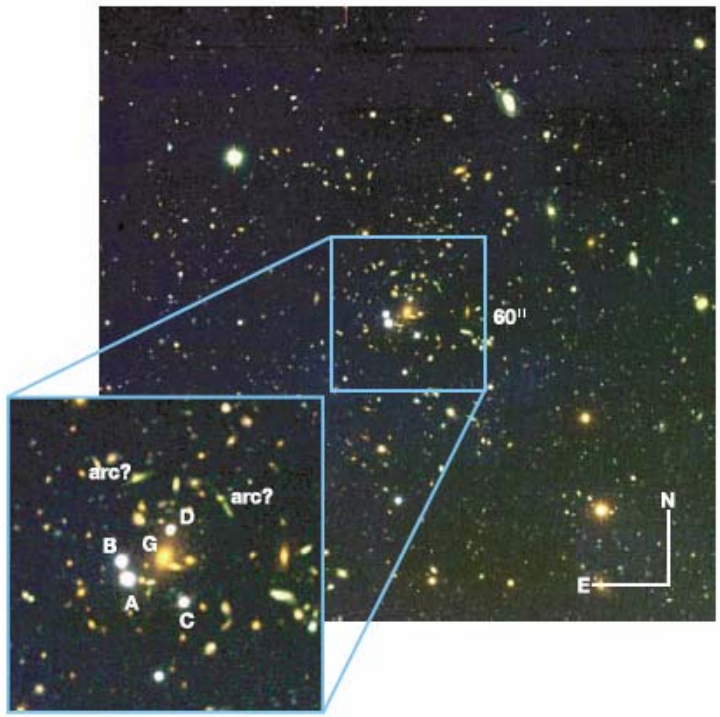

Figure 2 The *gri* composite Subaru image of the field around SDSS J1004+4112. The data were taken using the Subaru Prime Focus Camera[30] of the Subaru telescope. The magnitude limit is $i \approx 26.0$. The central 60″ square is shown in an expanded view. The four quasar components are marked as A, B, C and D, and the bright galaxy located between the four quasar components is marked as G. The separation between components A and D is 12.77″, and that between components B and C is 14.62″. The positions (J2000) and the magnitudes of the components A–D and the brightest galaxy (component G) between the four quasar components are summarized in Table 1. Many faint galaxies can be seen—their positions and colours are consistent with being members of a cluster ($z = 0.68$) centred on component G. Two possible arclets (marked as 'arc?') can also be seen. The seeing had a full-width at half-maximum of 0.6″.

Examlple of weak lensing: Abell 2218

D. Clowe et al., astro-ph/0608407

Merger of galaxy clusters

- Zwicky 1937: gravitational potentials of clusters of galaxies are too deep to be caused by baryonic mass
- Oort 1932: Non-luminous “dark matter”
- On-going galaxy cluster merger: observed baryons and the inferred dark matter are spatially segregated, since
  - dark matter are collisionless particles
  - the fluid-like X-ray emitting intracluster plasma experiences ram pressure.

1E0657-558: optical image

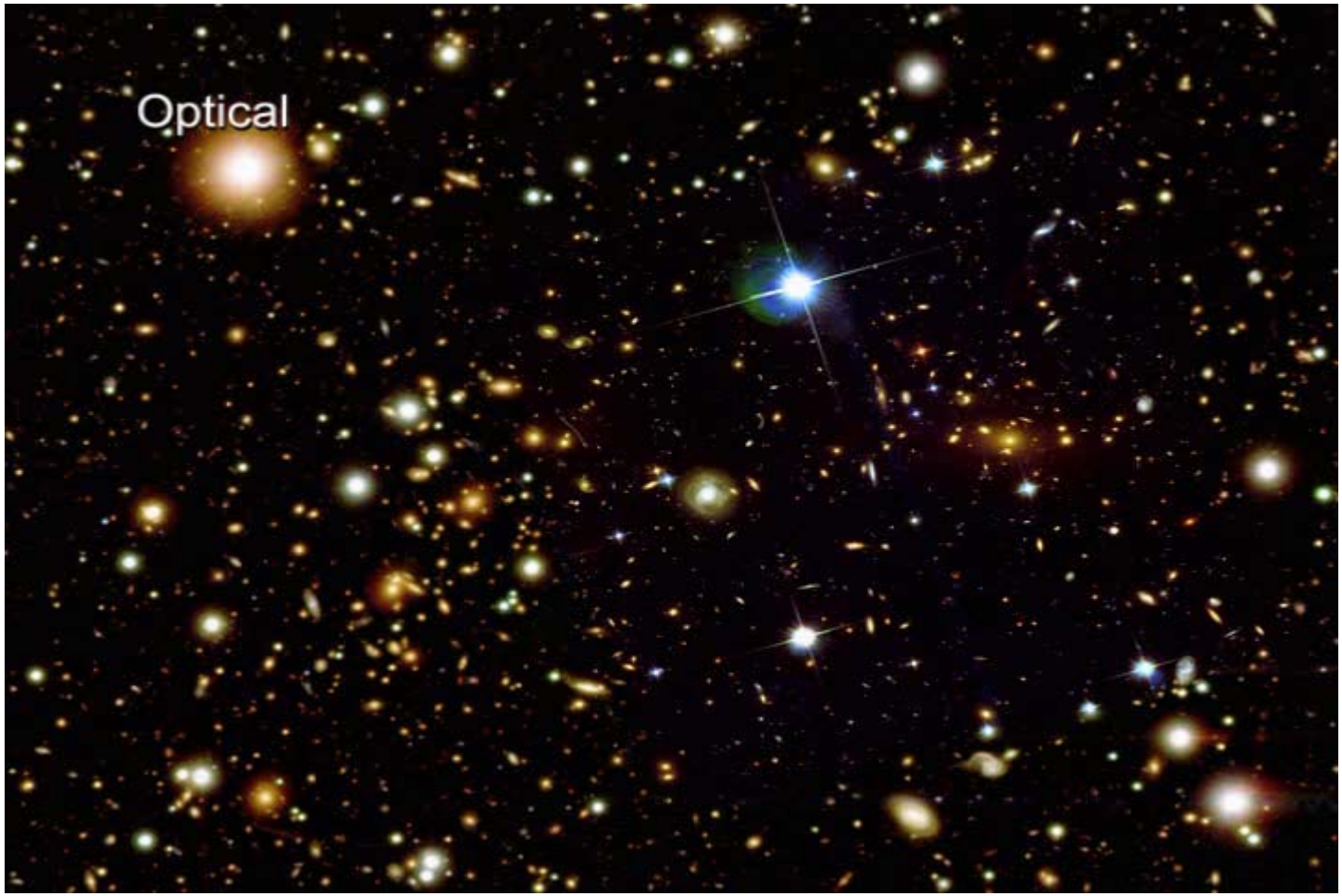

Z=0.296

7.5 x 5.4 arcmin image by Magellan (Two 6.5m Telescopes at Las Campanas Observatory)

D. Clowe et al., astro-ph/0608407

Weak gravitational lensing

- Measure orientation and extension of galaxies
- Shear $\vec{\gamma}$: amount of anisotropic stretching of the galaxy image
- Corrected ellipiticity (or reduced shear, measured $\vec{g} = \vec{\gamma}/(1-\kappa)$
- Map of κ

$$\nabla \ln(1-\kappa) = \frac{1}{1-g_1^2-g_2^2}\begin{pmatrix} 1+g_1 & 1+g_2 \\ g_2 & 1-g_1 \end{pmatrix}\begin{pmatrix} g_{1,1}+g_{2,2} \\ g_{2,1}-g_{1,2} \end{pmatrix}$$

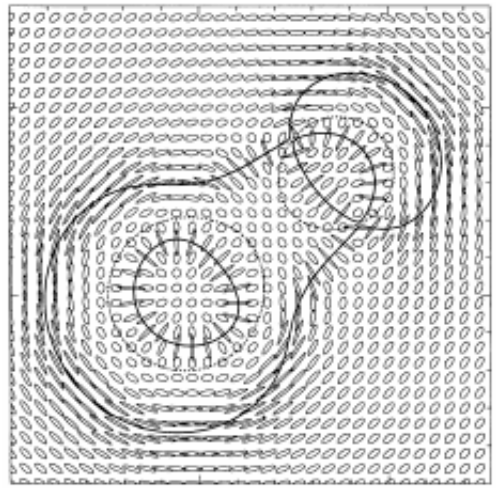

(Including derivatives of (g_1, g_2):

Kaiser 1995, Schneider 1995)

2.2. Weak lensing analysis

The goal of weak lensing analysis of a cluster field is to determine the convergence, κ, across the field, which is related to the surface mass density, Σ, via

$$\kappa = \frac{\Sigma}{\Sigma_{\rm crit}}. \quad (1)$$

$\Sigma_{\rm crit}$ is a scaling factor:

$$\Sigma_{\rm crit}^{-1} = \frac{4\pi G}{c^2}\frac{D_{\rm ol} D_{\rm ls}}{D_{\rm os}} \quad (2)$$

where $D_{\rm os}$ is the angular distance from the observer to the source (background) galaxy, $D_{\rm ol}$ is the angular distance from the observer to the lens (cluster), and $D_{\rm ls}$ is the angular distance from the lens to the source galaxy. With knowledge of the redshift of the cluster, redshift distribution of the background galaxies used to derive κ, and a chosen cosmology, one can convert a κ distribution into a surface mass density distribution for the cluster. What is measured from the background galaxies, however, is the reduced shear

$$\boldsymbol{g} = \frac{\boldsymbol{\gamma}}{1-\kappa} \quad (3)$$

which is a function of both the convergence and the gravitational shear, $\boldsymbol{\gamma}$. To convert the measured reduced shear field around the clusters to a κ distribution, we use three different methods.

Clowe et al., AA 451, 395 (2006)

both κ and γ are combinations of second derivatives of the surface potential, and therefore

$$\nabla \ln(1-\kappa) = \frac{1}{1-g_1^2-g_2^2} \begin{pmatrix} 1+g_1 & g_2 \\ g_2 & 1-g_1 \end{pmatrix} \begin{pmatrix} g_{1,1}+g_{2,2} \\ g_{2,1}-g_{1,2} \end{pmatrix} \quad (4)$$

(Kaiser 1995), and solves for $\ln(1-\kappa)$ within a field except for an unknown additive constant. The technique also requires a continuous field for both $\boldsymbol{g}$ and its first derivative, which we created by using a regularly spaced grid for the shear field, with the shear value at each position being the weighted mean of the shear values of the surrounding galaxies. The weighting function used was

$$w = \exp\left(\frac{d^2}{2d_0^2}\right) \times \min(\nu_t, 40) \quad (5)$$

where d is the distance between the grid point and the galaxy, d_0 is the chosen smoothing length (25.″6 for the reconstructions shown in Figs. 2–21), and ν_t is the sum in quadrature of the significances in each passband. The 25.″6 smoothing length for the reconstructions shown in the figures was chosen as a compromise between wanting to suppress small-scale noise peaks in the mass reconstructions while also preserving the shape of the mass distribution of the clusters in the inner few hundred kpc.

Clowe et al., AA 451, 395 (2006)

D. Clowe et al., astro-ph/0608407

Optical + dark matter

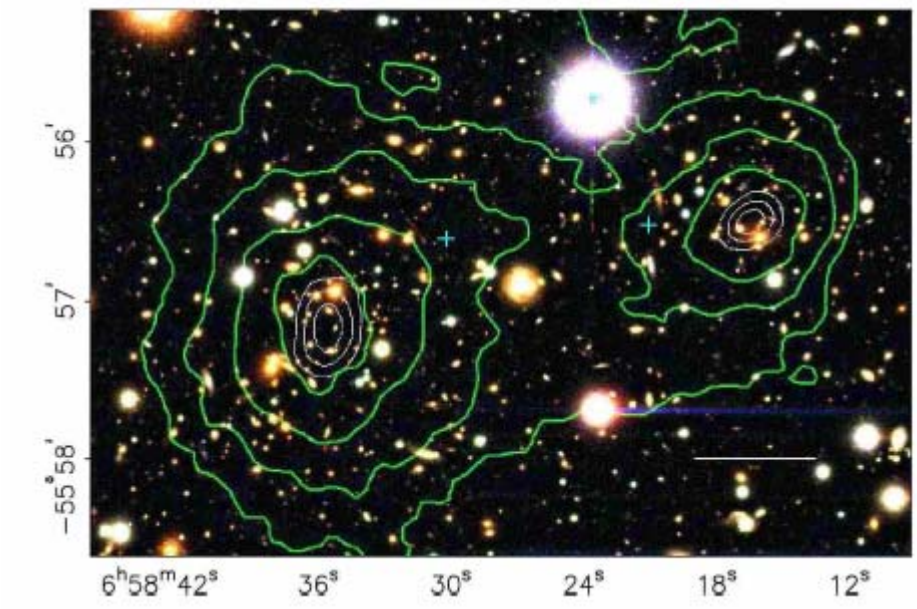

Color image from the Magellan images of the merging cluster 1E0657−558, with the white bar indicating 200 kpc at the distance of the cluster. Shown in green contours in both panels are the weak lensing κ reconstruction with the outer contour level at $\kappa = 0.16$ and increasing in steps of 0.07. The white contours show the errors on the positions of the κ peaks and correspond to 68.3%, 95.5%, and 99.7% confidence levels. The blue +s show the location of the centers used to measure the masses of the plasma clouds.

1E0657-558: dark matter

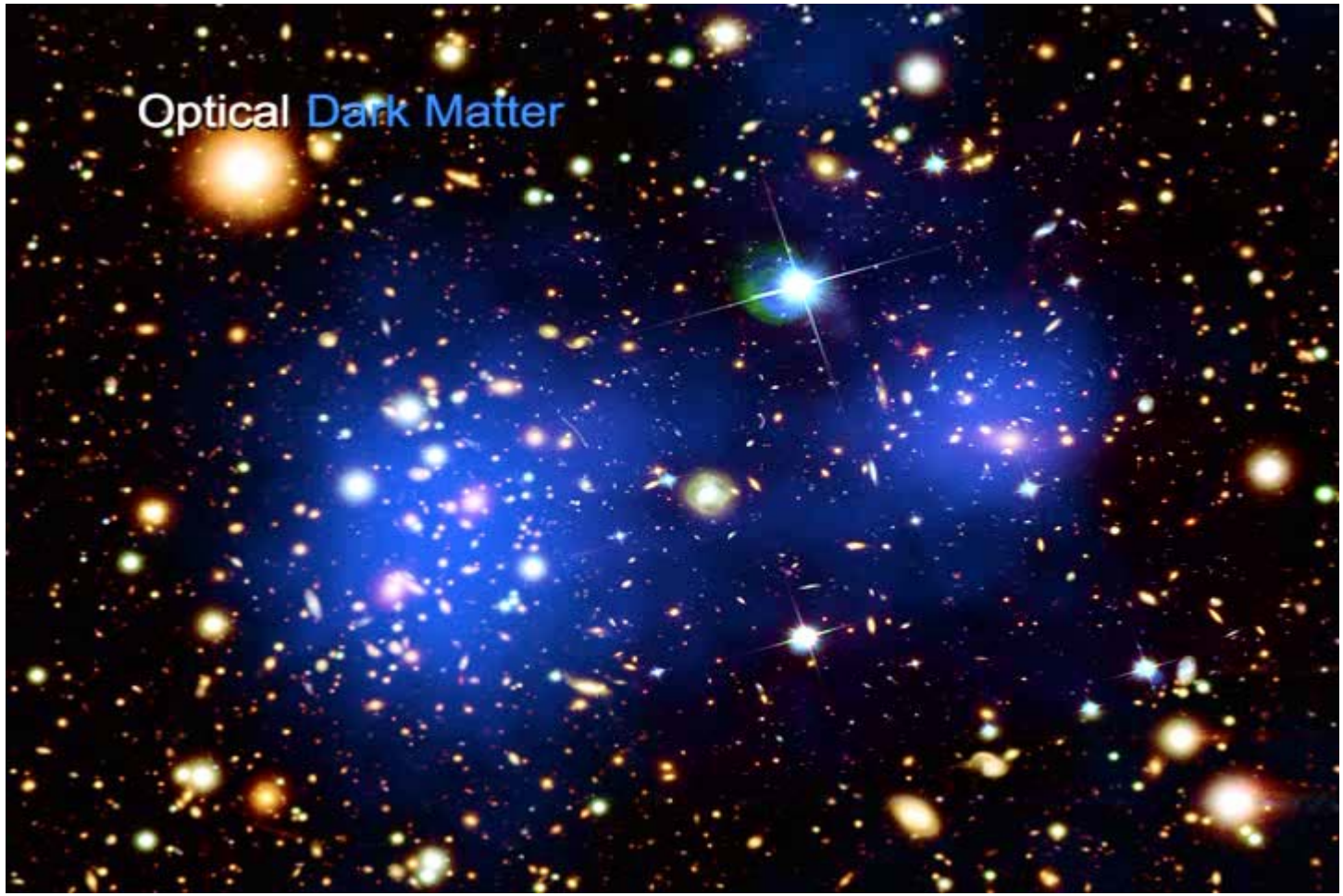

D. Clowe et al., astro-ph/0608407

X-ray + dark matter

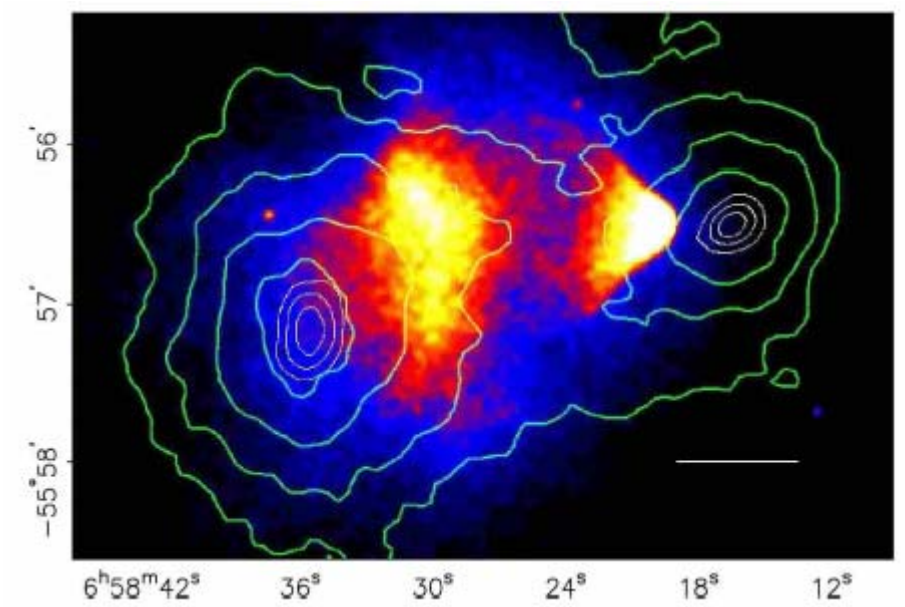

500 ks Chandra image of the cluster. Shown in green contours in both panels are the weak lensing κ reconstruction with the outer contour level at κ = 0.16 and increasing in steps of 0.07. The white contours show the errors on the positions of the κ peaks and correspond to 68.3%, 95.5%, and 99.7% confidence levels. The blue +s show the location of the centers used to measure the masses of the plasma clouds.

1E0657-558: optical+X-ray

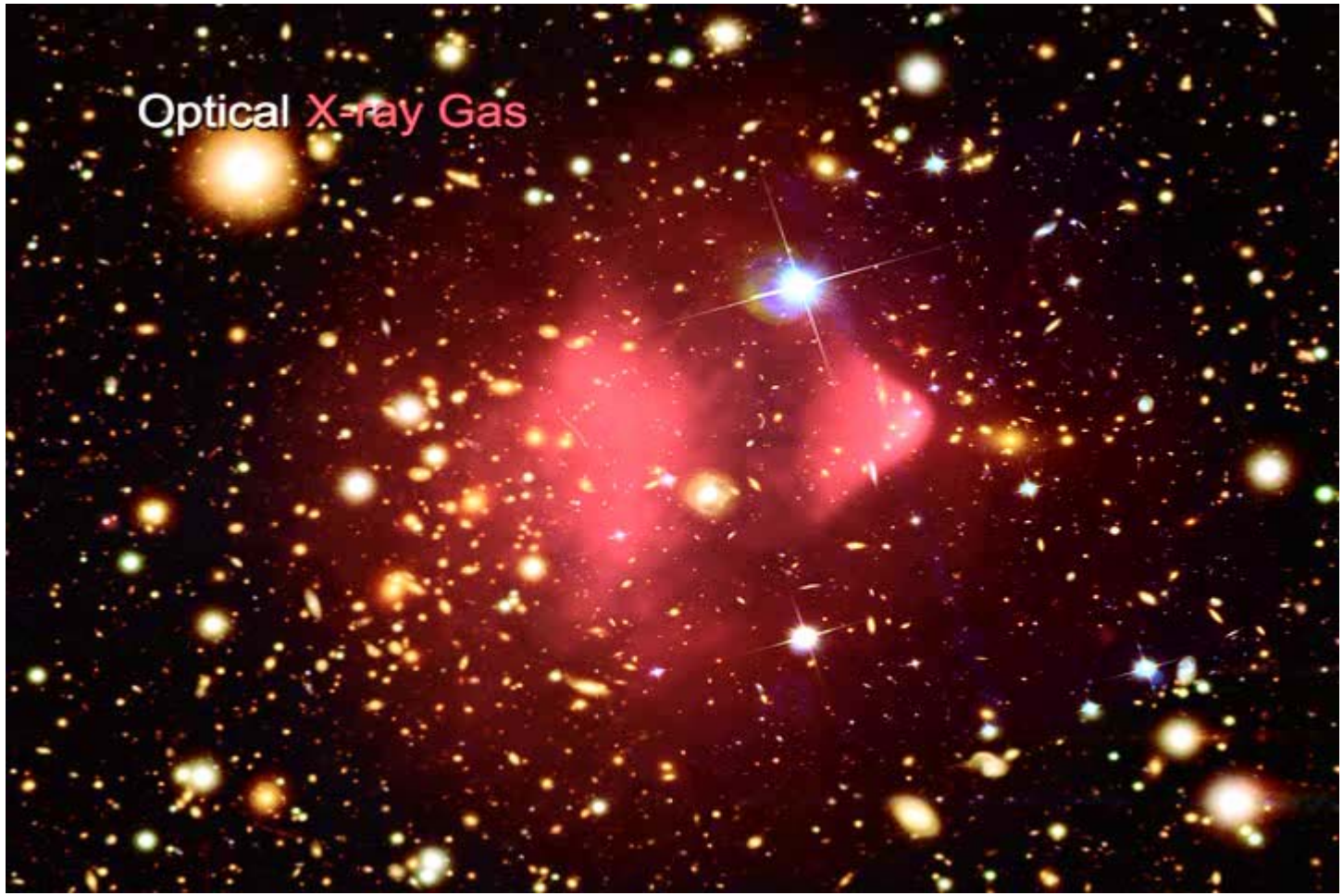

Optical+darkmatter+X-ray

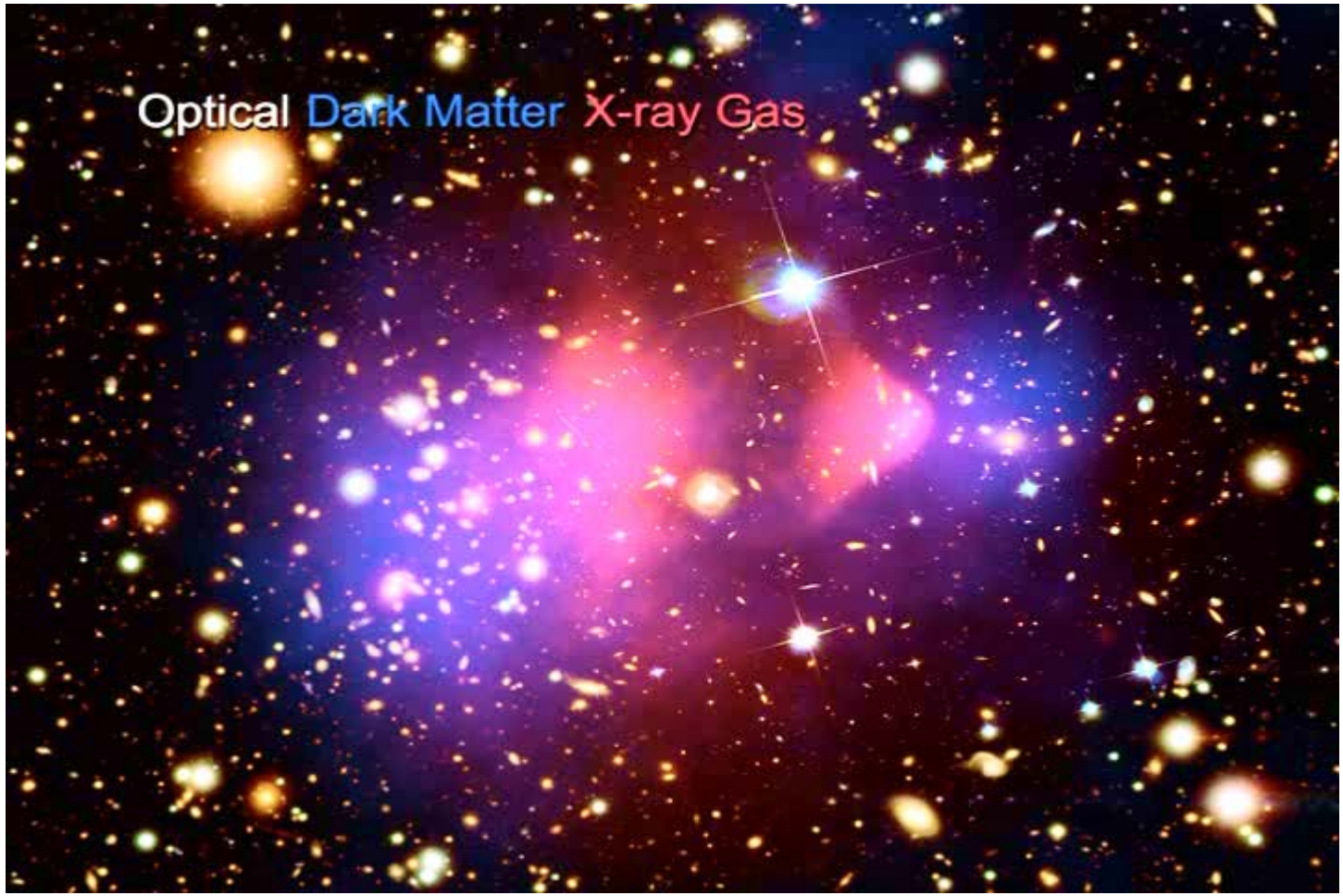

http://chandra.harvard.edu/photo/2006/1e0657/animations.html

1E0657-558: animation

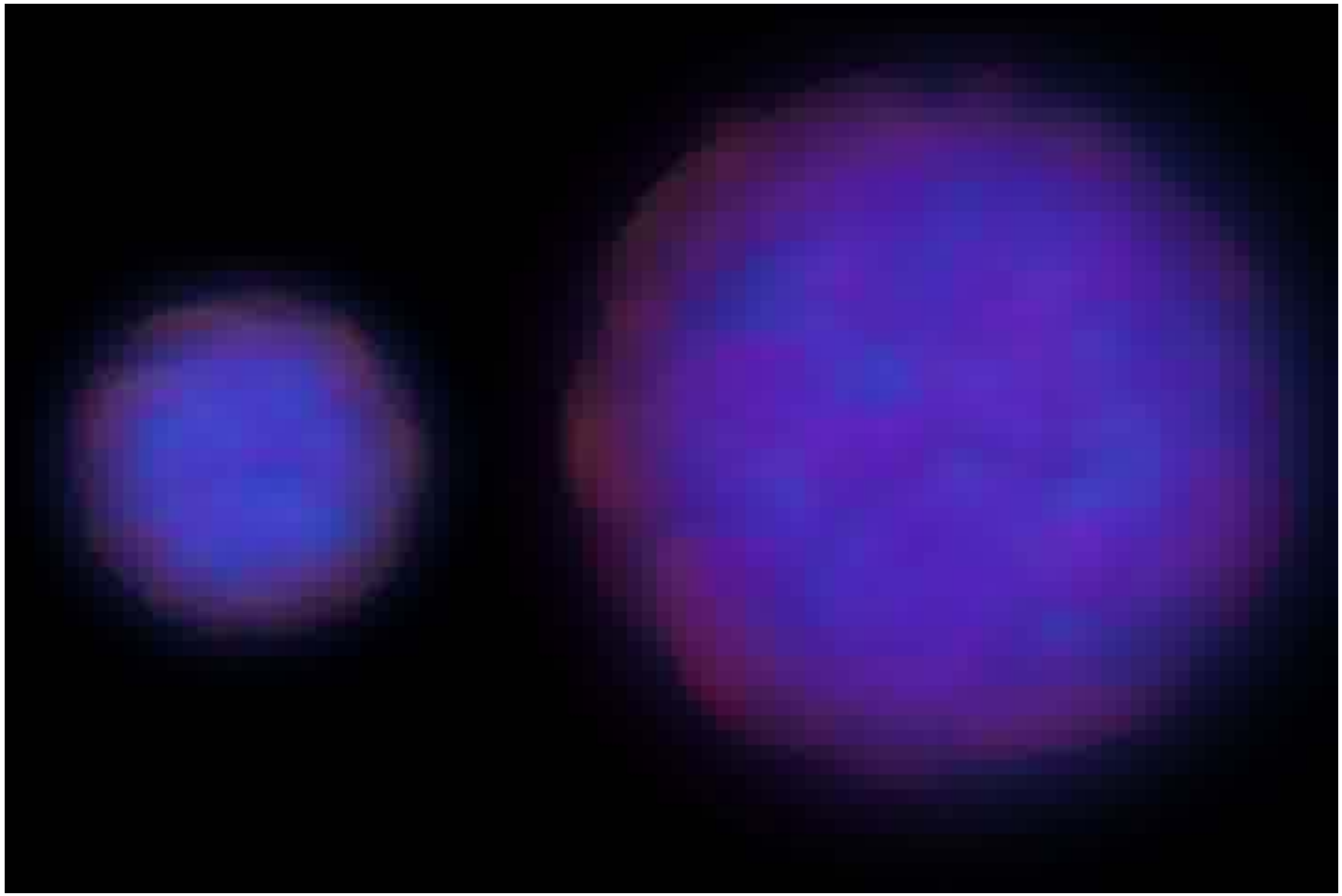

http://chandra.harvard.edu/photo/2006/1e0657/animations.html

1E0657-558: 3D animation

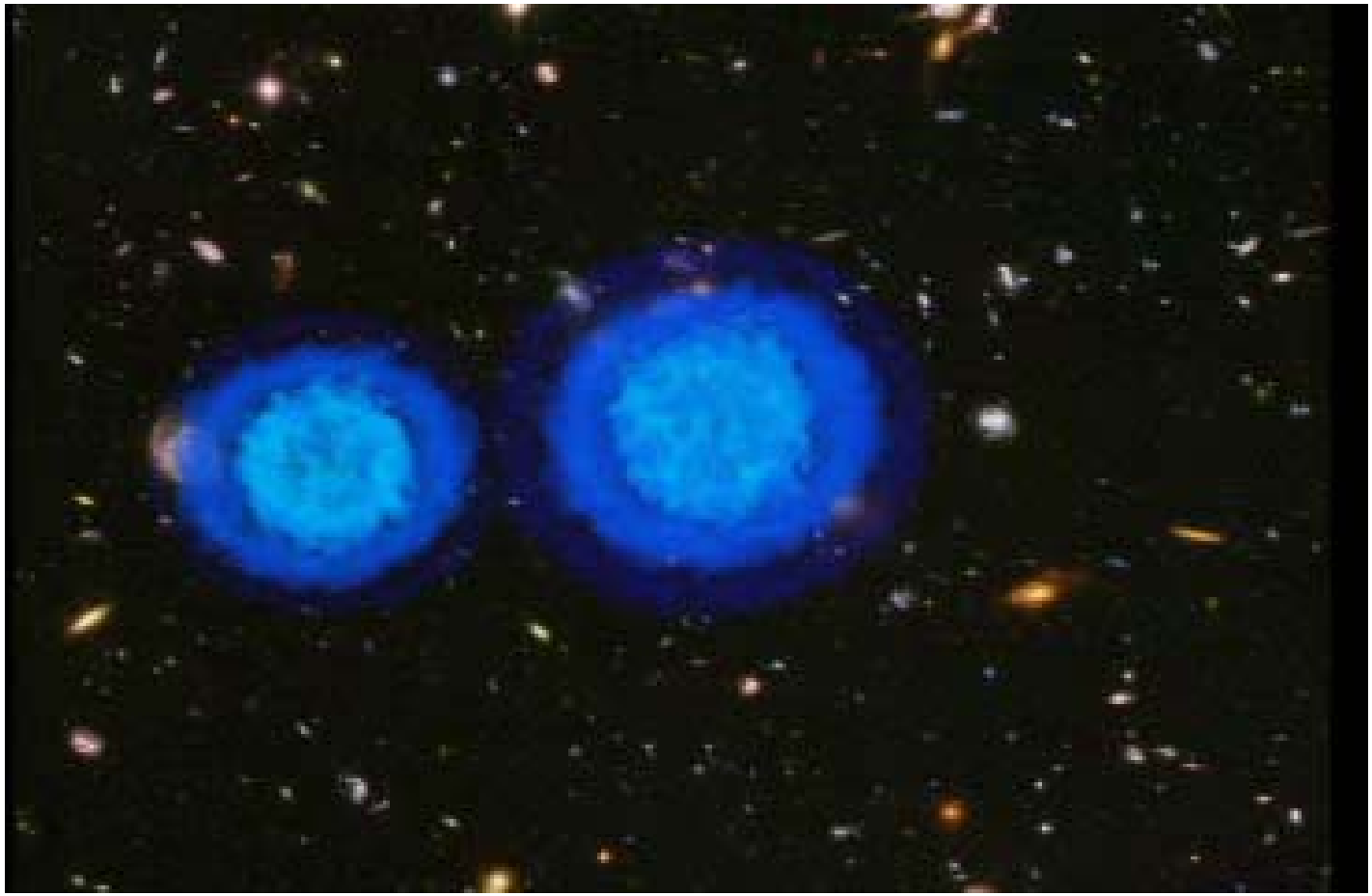

D. Clowe et al., astro-ph/0608407

TABLE 1
OPTICAL IMAGING SETS

Instrument	Date of Obs.	FoV	Passband	t_{exp} (s)	m_{lim}	n_d ($'^{-2}$)	seeing
2.2m ESO/MPG	01/2004	$34' \times 34'$	R	14100	23.9	15	$0\farcs8$
Wide Field Imager	01/2004		B	6580			$1\farcs0$
	01/2004		V	5640			$0\farcs9$
6.5m Magellan	01/15/2004	$8'$ radius	R	10800	25.1	35	$0\farcs6$
IMACS	01/15/2004		B	2700			$0\farcs9$
	01/15/2004		V	2400			$0\farcs8$
HST ACS	10/21/2004	$3\farcm5 \times 3\farcm5$	F814W	4944	27.6	87	$0\farcs12$
subcluster	10/21/2004		F435W	2420			$0\farcs12$
	10/21/2004		F606W	2336			$0\farcs12$
main cluster	10/21/2004	$3\farcm5 \times 3\farcm5$	F606W	2336	26.1	54	$0\farcs12$

NOTE. — Limiting magnitudes for completion are given for galaxies and measured by where the number counts depart from a power law. All image sets had objects detected in the reddest passband available.

TABLE 2
COMPONENT MASSES

BCG: Brightest Cluster Galaxy

Component	RA (J2000)	Dec (J2000)	$M_X (10^{12} M_\odot)$	$M_* (10^{12} M_\odot)$	$\bar{\kappa}$
Main cluster BCG	06 : 58 : 35.3	−55 : 56 : 56.3	5.5 ± 0.6	0.54 ± 0.08	0.36 ± 0.06
Main cluster plasma	06 : 58 : 30.2	−55 : 56 : 35.9	6.6 ± 0.7	0.23 ± 0.02	0.05 ± 0.06
Subcluster BCG	06 : 58 : 16.0	−55 : 56 : 35.1	2.7 ± 0.3	0.58 ± 0.09	0.20 ± 0.05
Subcluster plasma	06 : 58 : 21.2	−55 : 56 : 30.0	5.8 ± 0.6	0.12 ± 0.01	0.02 ± 0.06

NOTE. — All values are calculated by averaging over an aperture of 100 kpc radius around the given position (marked with blue +s for the centers of the plasma clouds in Fig 1). $\bar{\kappa}$ measurements for the plasma clouds are the residual left over after subtraction of circularly symmetric profiles centered on the BCGs.

An 8σ significance spatial offset of the center of the total mass from the center of the baryonic mass peaks!

Modified gravitational force law (1)

- Modified gravity (MOG) can describe lensing without postulating dark matter.

$$a(r) \equiv \frac{d\Phi(r)}{dr} = -\frac{G(r)M(r)}{r^2}$$

$$G(r) = G_N\left[1+\alpha(r)(1-\exp(-r/\lambda(r)))\left(1+r/\lambda(r)\right)\right]$$

- G_N: Newton' const, $\alpha(r)$: running coupling strength, $\lambda(r)$: range of the vector "phion" field
- $G_\infty \rightarrow G_N\,(1+\alpha)$ as $r \rightarrow \infty$, $G(r) \rightarrow G_N$ as $r \rightarrow 0$

Moffat, astro-ph/0608675

Modified gravitational force law (2)

$$\kappa(R) = \frac{4\pi G_N D}{c^2}\left[1 + \alpha_{\rm clust}(1 - \exp(-R/\lambda_{\rm clust}))\left(1 + \frac{R}{\lambda_{\rm clust}}\right)\right]\Sigma(R).$$

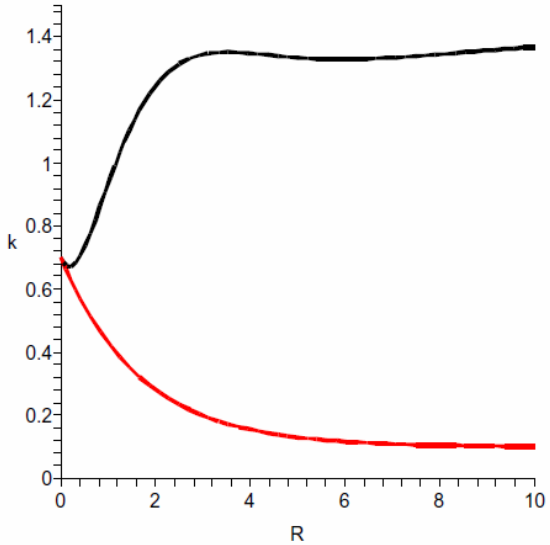

Figure 1.

Shown is a calculation of the convergence field $\kappa(R)$ for a spherically symmetric model of the interacting cluster. The MOG result is displayed by a black curve and the Einstein (Newtonian) result by a red curve. The vertical axis is displayed with the constant numerical factor $4\pi G_N D/c^2$ scaled to unity in appropriate units and the horizontal axis $R = 100 \times$ kpc.

"We see that the MOG prediction for the gravitational convergence field κ (R) displays the peaking of the weak lensing in the outer regions of the interacting cluster relative to the peaking of the central off-set X-ray gas without dark matter."

Summary

- Dark matter distribution of merging galaxy clusters, 1E0657-558, was reconstructed by use of weak lensing.
- It does not trace the plasma distribution which is the main baryonic component derived by X-rays, but traces galaxy distribution where dark matter is ruling.
- Majority of matter in the system is unseen!
- Or modified gravitational force law can explain?